Linked Knots from the *gyro* Operation on the Dodecahedron

Henriette Lipschütz[1], Martin Skrodzki[2], Ulrich Reitebuch[3], and Konrad Polthier[4]

[1]Institut für Mathematik, Freie Universität, Berlin, Germany; henriette.lipschuetz@fu-berlin.de
[2]CGV group, TU Delft, Delft, the Netherlands; mail@ms-math-computer.science
[3]Institut für Mathematik, Freie Universität, Berlin, Germany; ulrich.reitebuch@fu-berlin.de
[4]Institut für Mathematik, Freie Universität, Berlin, Germany; konrad.polthier@fu-berlin.de

Abstract

John Horton Conway's taxonomy for Archimedean and Catalan solids includes the snub and the dual operation, their combination being known as the *gyro* operation. Intriguingly, recent work showed that the *gyro* operation can be used to create weaving patterns when applied to planar *n*-gons. This process can be applied to two-dimensional polyhedral surfaces in $\mathbb{R}^3$. In this paper, we investigate the weaving structures that are created on the dodecahedron. We show that the weaving structures can be interpreted via knot theory and written in form of a link diagram. Furthermore, we prove the number of knots arising on the dodecahedron to be six. Finally, we present hand-crafted physical representations of the results in form of balls made of yarn, inspired by Japanese temari.

1 Conway's *dual-snub* or Hart's *gyro*

In their influential book "The Symmetries of Things" [2], John Horton Conway and his co-authors introduce a naming scheme for the Archimedean and Catalan solids. Together with Platonic solids, these three collections of polyhedra enchant in many contexts with their regularity properties. While all Platonic and Catalan solids consist of a single face type (they are face-transitive), the Archimedean solids consist of up to three different face types. The Platonic and Archimedean solids have in common that their vertices are vertex-uniform, which is not true for the Catalan solids. Each Catalan solid possesses at least two different vertex configurations. These three families of solids are closely related. Each Archimedean solid can be derived from a Platonic solid by elementary operations like truncation, expansion, rectification, or alternation. The Catalan and Archimedean solids are dual to each other.

For example, the snub dodecahedron can be created from the dodecahedron using omnitruncation and alternation. First, all vertices and edges of the dodecahedron are truncated (so-called *omnitruncation*). This

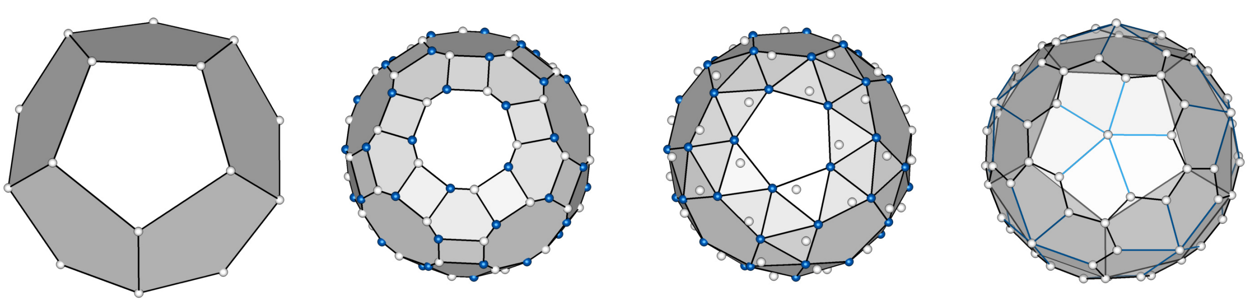

(a) *Dodecahedron.* **(b)** *Omnitruncation.* **(c)** *Alternation.* **(d)** *Dual.*

Figure 1: *Related solids.* ***(a)*** *dodecahedron;* ***(b)*** *omnitruncated dodecahedron with irregular faces, vertices alternatingly colored white and blue;* ***(c)*** *snub dodecahedron obtained by alternation;* ***(d)*** *the dual of the snub dodecahedron, the pentagonal hexecontahedron.*

leads to hexagons in place of vertices, rectangles in place of edges, and decagons in place of pentagonal faces, see Figure 1b. Afterwards every other vertex of every face is removed (so-called *alternation*). Thus, each decagon is cut to a pentagon, each hexagon to a triangle, and the gaps left by the removed parts are filled by new triangles, see Figure 1c. Note, to get a snub dodecahedron with regular faces, the omnitruncation step has to be performed with slightly irregular faces. Now, taking the dual of the snub dodecahedron gives the pentagonal hexecontahedron, noted down as $\mathtt{P}_{60}$ by Conway et al., see Figure 1d. The steps described here correspond to forming the dual of the snub dodecahedron. George Hart collects an expansion of Conway's taxonomy on a website [3]. There, the process explained above corresponds to the *gyro* operation which consists of dualizing (d) a snub (s) polyhedron processed on the dodecahedron noted as dsD = gD by George Hart. In the following, we will stick with the notation as *gyro* operation and use $\mathtt{g}^n\mathtt{P}$ to denote how often the *gyro* operation was applied to the considered polyhedron P.

When comparing the pentagonal hexecontahedron with the dodecahedron, it can be observed that a part of the *gyro* operation replaces every edge of the dodecahedron by three edges in order to arrive at the pentagonal hexecontahedron. Additionally, a vertex is added to each face of the dodecahedron. Now, choosing an orientation of an arbitrary face f provides an order of its edges and thus an order of the two new vertices introduced on each edge e of the original dodecahedron. The first of these vertices—according to the chosen order—is then connected to the vertex introduced above f while the other is connected to the vertex above the face that is adjacent to f via e. Note that the chosen order thereby propagates across all faces. This results in replacing every pentagonal face of the dodecahedron by five pentagons.

2 A Geometric Realization of the *gyro* Operation

The *gyro* operation as introduced by Conway and Hart is purely combinatorial. However, Figure 1 depicts a geometric realization of applying the *gyro* operation to the dodecahedron once. In the following, we will discuss how to obtain a geometric embedding of the combinatorial structure that arises when applying the *gyro* operation an arbitrary number of times to an arbitrary polyhedron P.

To find such a geometric embedding, several iterative methods are available, see [7, p. 119]. A corresponding mechanism has been implemented by George Hart on his website [3]. This uses the fact that planar three-connected graphs—such as the ones made from applying the *gyro* operation—can be used to build a three-polytope whose edges are all tangent to the unit sphere such that the origin is the barycenter of the contact points, see [7, Theorem 4.13]. Resulting geometric embeddings of iterative applications of the *gyro* operation to the dodecahedron are shown in Figure 2. As you can see, the edges form an intricate pattern, which has been discussed in the two-dimensional case, see [4]. However, in this paper, we are rather interested in structures that arise from coloring the faces.

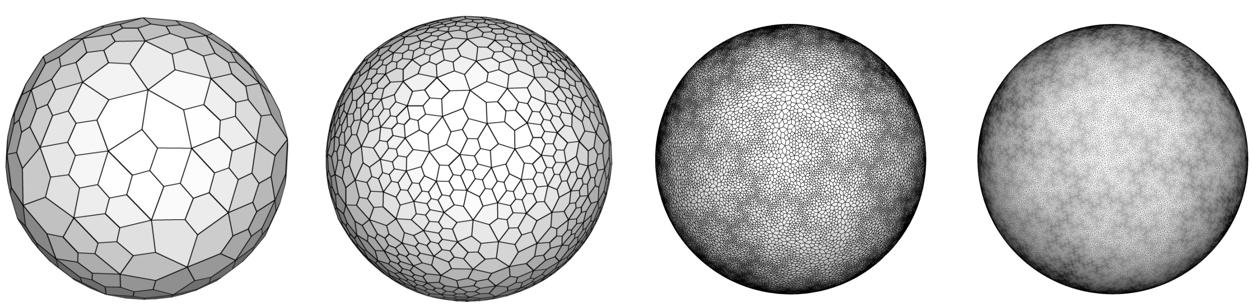

(a) $\mathtt{g}^2\mathtt{D}$. **(b)** $\mathtt{g}^3\mathtt{D}$. **(c)** $\mathtt{g}^5\mathtt{D}$. **(d)** $\mathtt{g}^6\mathtt{D}$.

Figure 2: *Iterative applications of the* gyro *operation to the dodecahedron* D.

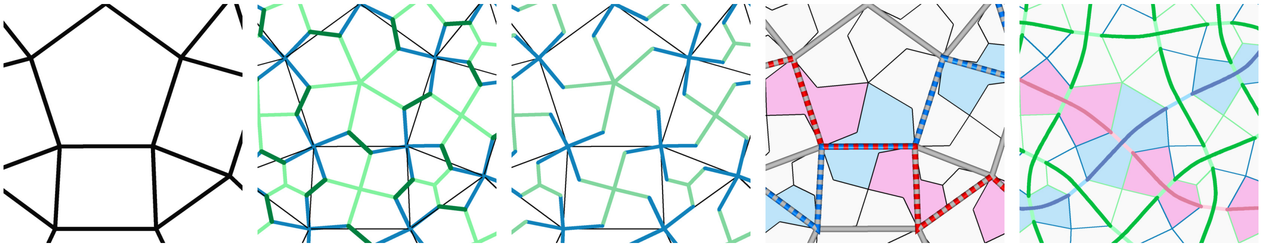

(a) *Arrangement of irregular n-gons.* **(b)** *Applying* gyro *opertation.* **(c)** *Pentagons joined to octagons.* **(d)** *Two Petrie walks (dashed).* **(e)** *Emergence of a weaving pattern.*

Figure 3: *Construction of weaving patterns. **(a)** input faces; **(b)** first and last edges of Z-triplets are colored in blue, middle edges in dark green; **(c)** octagons from removing middle edges; **(d)** Petrie walks on input faces shown as dashed lines; **(e)** weaving pattern.*

3 The Emergence of Weaving Structures

When considering the illustration from the beginning, we can note that each edge of the original dodecahedron is replaced by a Z-shaped path of four vertices and three edges, compare Figures 1a, 1d, and 3b. Henceforth, we will call such path a *Z-triplet*. Note that every pentagon we obtained from the *gyro* operation contains exactly one middle edge of such a Z-triplet. Furthermore, the opposing vertex belongs to the middle edge of another Z-triplet; this edge is not part of the pentagon considered. This has previously been noted by the authors in a different setting, see [4]. There, this observation is used to create weavings. In the following, we will follow their procedure. When the middle edge e_m of each Z-triplet is deleted, the two pentagons adjacent to e_m are merged into an irregular octagon. The octagons will then be used to create a weaving structure, which is illustrated in Figure 3 and which will be explained in detail in the remainder of this section.

As described above, the *gyro* operation replaces an original face by as many irregular pentagons as the face had vertices, compare Figures 3a and 3b. After deleting the middle edges of the Z-triplets, two pentagons are joined into an octagon, see Figure 3c. Then, every octagon O is surrounded by four octagons, each containing a green and a blue consecutive edge from O, see Figure 3c. Now, fix a single octagon O and consider the adjacent octagons, which lie opposite to each other, in two pairs. Then, the deleted middle edges of O and the middle edges of the neighboring octagons form the following patterns: and , showing the pink strand passing over the blue ones and under the green ones. Here, the deleted middle edges

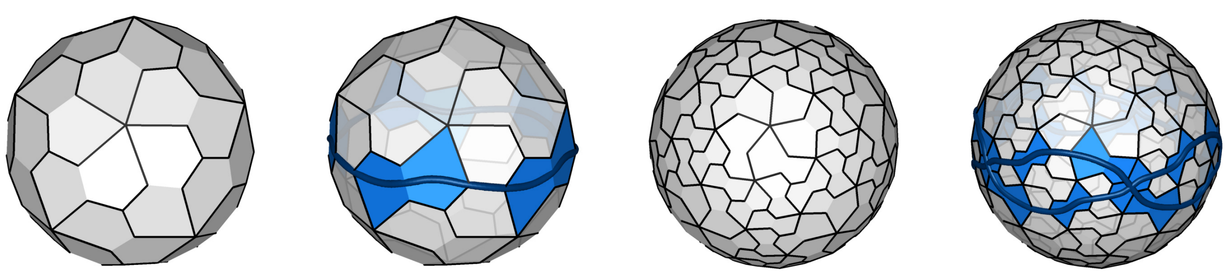

(a) *Octagons on* gD. **(b)** *Coloring a weaving strand.* **(c)** *Octagons on* g^{2}D. **(d)** *A strand from* g^{2}D *winds around twice.*

Figure 4: *Octagons on* gD *and* g^{2}D*. **(a)** octagons on* gD *by grouping pairs of pentagons from* gD*, compare Figure 1d; **(b)** single weaving strand colored in blue; **(c)** octagons from* g^{2}D*, compare leftmost image of Figure 2; **(d)** knot on* g^{2}D *with five crossings colored in blue.*

of the octagons indicate a strand which passes over (blue) and under (pink) the central octagon O. This can be observed when focusing on the central blue octagon O in Figure 3e. These strands can be interpreted as forming a structure similar to that of a warp and weft weaving.

As discussed in Section 1 and shown in Figure 1, the *gyro* operation can be applied to the dodecahedron. To create the weaving structure on the result, all middle edges of the Z-triplets are removed. This merges pairs of pentagons into irregular and non-planar octagons, see Figure 4a. Here, each of the twelve original pentagonal faces of the dodecahedron is split into five irregular ones, which yields 60 irregular pentagons. Those are paired up to form 30 octagons. We create a strand by starting at an arbitrary octagon and following the deleted middle edges to the next, iteratively. The resulting weaving strands on these octagons, when constructed according to Figure 3e, then start to wind around the dodecahedron, see Figure 4b.

Each of these strands crosses a closed path of edges on the dodecahedron, turning alternatingly left and right at vertices, a so-called *Petrie walk* [5], see Figure 3d. On the dodecahedron, each Petrie walk consists of ten edges. Since each edge is crossed by two strands, we can interpret this as the strand passing alternatingly over and under the Petrie walk. The strands close and there are six in total, covering five octagons each, on gD. As they close in on themselves, we will refer to them as *knots* and explore this relation in the following.

4 Knots and Links

We have seen that the emerging weaving structure on gD forms strands that close in on themselves and thus form knots, see Figure 4b. In mathematics, a *knot* is a simple closed curve $\kappa : [0, 1] \to \mathbb{R}^3$. Two knots are said to be *equivalent* if there exists an orientation-preserving homeomorphism from one knot to the other. Intuitively, one can think of the knot as made of a circular string. Then, two knots are equivalent if one can move the string representing one knot, without gluing or cutting it, to transform it into the other. To study knots, *knot diagrams* are used, which arise from projecting a knot onto the plane and displaying the behavior at the crossings. Several entangled knots are called a *link* and their projection is called a *link diagram*.

The procedure outlined above gives rise to several knots on gD, with one such knot shown in Figure 4b. When coloring in all such knots on gD, there are six pairwise equivalent knots, see Figure 5a. Note that each of these knots is a simple circle, i.e., equivalent to the unknot. In Figure 5a, to get a better understanding of the structure of the link based on the *gyro* operation, the dodecahedron as well as all vertices and edges arising from application of the *gyro* operation are projected centrally to the sphere. Instead of considering the octagons as introduced before, every octagon is now represented by a linear segment orthogonal to the deleted middle edge of the Z-triplets that gave rise to the octagon. Now, these line segments represent the linked

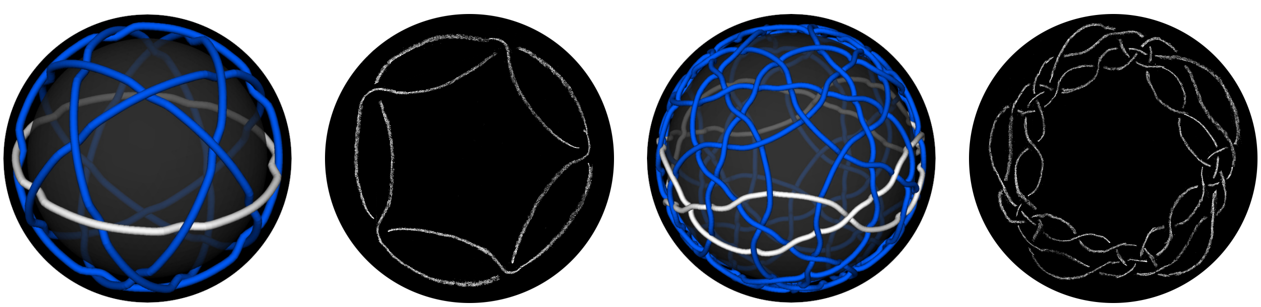

(a) *Weaving structure knots from* gD. **(b)** *Knot diagram of a single knot of* g^2D. **(c)** *Weaving structure knots from* g^2D. **(d)** *Knot diagram of a single knot of* g^3D.

Figure 5: *Link and knots from the* gyro *operation applied to the dodecahedron.* ***(a)*** *link consisting of six (un-)knots on* gD*;* ***(b)*** *knot diagram of a single knot from* g^2D*;* ***(c)*** *link of six knots on* g^2D*;* ***(d)*** *knot diagram of a single knot from* g^3D.

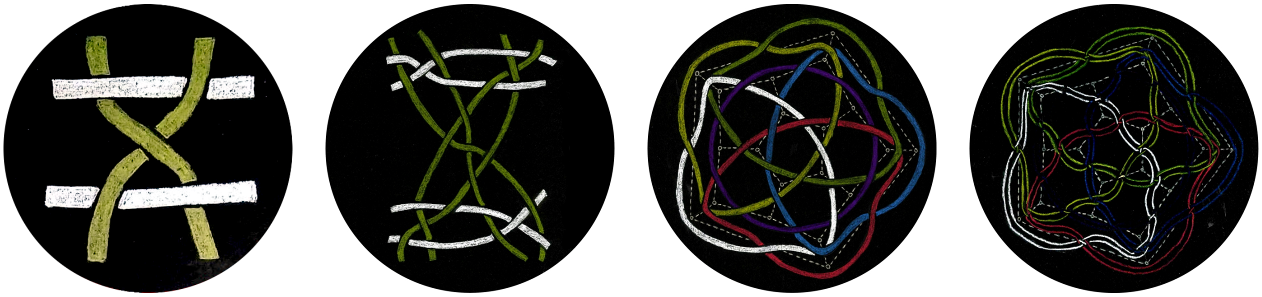

(a) $\mathtt{g}^2\mathtt{D}$ *link block.* **(b)** $\mathtt{g}^3\mathtt{D}$ *link block.* **(c)** $\mathtt{gD}$ *link diagram.* **(d)** $\mathtt{g}^2\mathtt{D}$ *link diagram.*

Figure 6: ***(a)*** *link block level 2;* ***(b)*** *link block level 3; flattened edges of the dodecahedron with overlying linked knots* ***(c)*** *level 1 and* ***(d)*** *level 2. Note how the lower levels transform into the higher ones.*

knots. On $\mathtt{gD}$, the six (un-)knots lie on six great circles and correspond to the edges of an icosidodecahedron projected to the sphere. The crossings of the six knots fall onto the vertices of the icosidodecahedron. Every single knot crosses all other five exactly twice, see the link diagram in Figure 6c. Running along a fixed knot shows that passing under and over one of the other knots takes place alternately. Hence, the crossings of two knots lie on antipodal points on the sphere. For one of these knots, it passes first over and then under the other one. Hence, the two knots indeed form a link and so do the five knots on $\mathtt{gD}$.

Now, we will consider what happens when applying the *gyro* operation twice to the dodecahedron. That is, how will the weaving structure on $\mathtt{g}^2\mathtt{D}$ look in relation to that on $\mathtt{gD}$? For this, consider $\mathtt{g}^2\mathtt{D}$ as shown in Figure 4c and a single strand of the weaving as shown colored in Figure 4d.

First, we observe that each knot wraps around the sphere twice now. When going from $\mathtt{D}$ to $\mathtt{g}^2\mathtt{D}$, for each knot κ, we replace those five crossings by the $\mathtt{g}^2\mathtt{D}$ link block shown in Figure 6a where κ is originally on top. That is, there is an uneven number of self-crossings, which results in the knot closing in on itself. It follows that it remains one knot that wraps around the sphere twice. Further, when going from $\mathtt{g}^n\mathtt{D}$ to $\mathtt{g}^{n+1}\mathtt{D}$, we perform the same operation on crossings between two different knots. However, for $n \geq 2$, we also replace each self-crossing of a knot with five self-crossings according to the link block shown in Figure 6b. That is, the originally uneven number of self-crossings is multiplied by an uneven number and thus remains uneven. Hence, the number of knots stays the same for any number of applications of the *gyro* operation.

Second, every crossing of two knots, as shown in Figure 5a is replaced by a *link block* of five crossings, see Figure 6a. That is, a crossing of two different knots is replaced by a self-crossing of the knot lying on top and four crossings of both knots such that they are passing alternately under and over each other. This results in the link diagram shown in Figure 6d representing the weaving structure on $\mathtt{g}^2\mathtt{D}$.

Note that when applying another *gyro* operation to reach $\mathtt{g}^3\mathtt{D}$ as shown in Figure 2, the first observation does not change. That is, the number of knots on $\mathtt{g}^n\mathtt{D}$ generally remains six for all $n \geq 1$. As for the second observation, the crossings become increasingly involved. When going from $\mathtt{g}^n\mathtt{D}$ to $\mathtt{g}^{n+1}\mathtt{D}$ for any $n \geq 2$, each crossing of two different knots is replaced, as before, by the link block as shown in Figure 6a. However, now self-crossings are also replaced. Namely, each self-crossing is replaced by five self-crossings such that the knot passes under and over itself alternatingly, see Figure 6b. These two replacement actions enable the creation of a link diagram of $\mathtt{g}^n\mathtt{D}$ for arbitrary $n \geq 3$.

5 Crafting Physical Realizations

Having discussed the underlying theory of the weaving structures on $\mathtt{g}^n\mathtt{D}$, we will now turn to the production of a physical realization of said weaving structure. We choose *temari* as artistic representations. The name derives from the Japanese characters *te* (手), meaning hand, and *mari* (鞠 or 毬), a ball. As opposed to kemari, kick-balls, temari are played with by hands and are softer, often artfully decorated. The embroideries on temari are based on symmetry groups such as those of the dodecahedron or icosahedron, see [6]. Additionally, they are decorated with motifs such as stars or cherry blossoms. Temari are assumed to have developed originally in China and were popular in the time period from 600 A.D. until 1300 A.D., see [1]. The inner part, which often consists of worn out fabric or rice grains, is wrapped with two layers of yarn—a thicker thread is wrapped around the inside to form the ball and then a thinner thread is used to cover the last layer completely. This last wrapping is now used as basis for the embroidery. When creating the embroidery, pins are stuck into the ball to mark the points of a net of help lines that is subsequently spanned between them. The positions of the pins can be found using paper strips with markings corresponding to regular subdivisions of a great circle. After constructing the net of help lines, the decorative patterns are embroidered into the outer layer.

Inspired by this technique, the following realizations of the weaving structures on $\mathtt{g}^n\mathtt{D}$ were realized. In contrast to the traditional technique described above, the decorations are not embroidered into the outer layer, but since the interwoven threads form six knots (for $\mathtt{gD}$), they simply lie on the surface. During manufacturing, the knots are kept in place using additional pins, see Figure 8. After completing all six knots, the link itself keeps them in place so that the pins can be removed.

First, the vertices of a dodecahedron are pinned on the ball and a net of help lines corresponding to the dodecahedron edges in a contrasting color is placed on the ball, see Figure 8a. Afterwards, the pins helping to keep one knot in place are distributed, see Figure 8b. Here, this results in two pins set slightly off the dodecahedron edges such that the crossing from another knot can be placed between them or it already

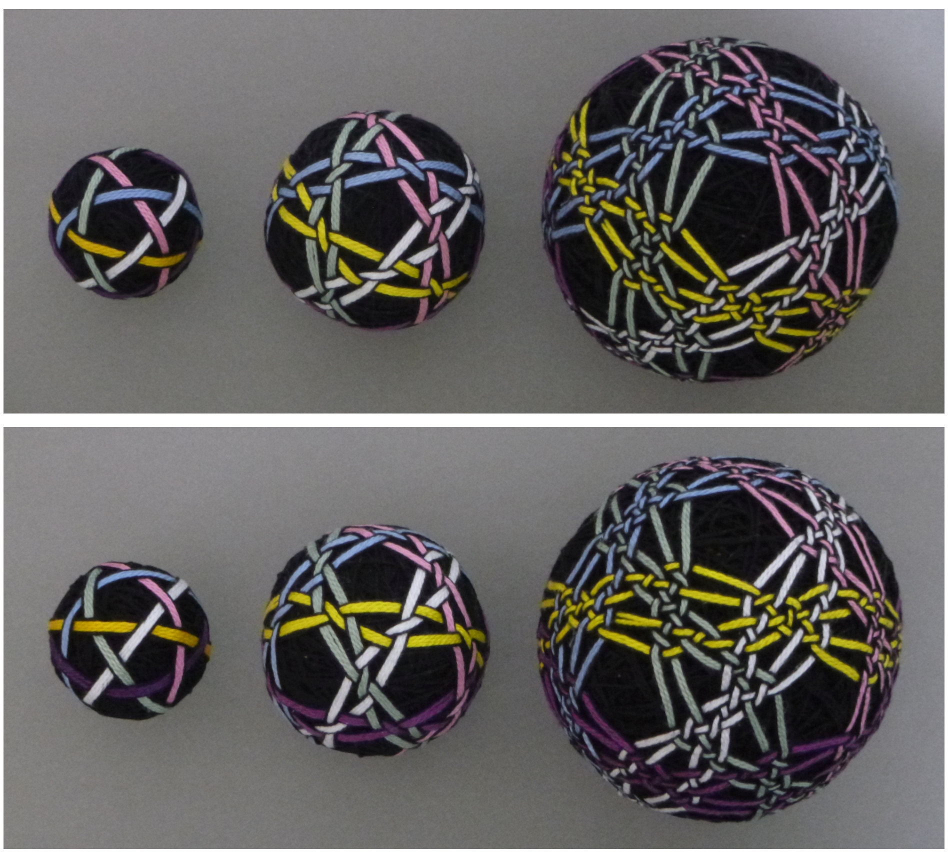

Figure 7: *Final result. From left to right: shown are the links corresponding to the first three iterative applications of the* gyro *operations* $\mathtt{gD}$, $\mathtt{g}^2\mathtt{D}$, *and* $\mathtt{g}^3\mathtt{D}$ *to the dodecahedron. The upper row focuses on the dodecahedral vertices, the lower row on the icosahedral vertices.*

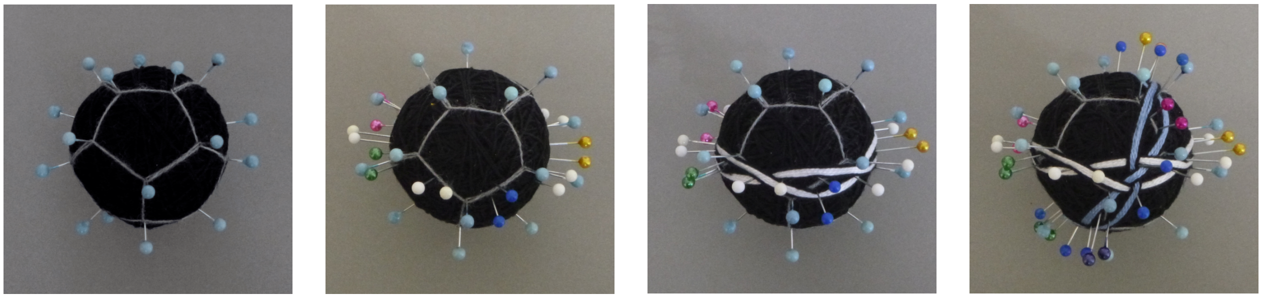

(a) D *structure.* **(b)** *Help-pins for one knot.* **(c)** *One knot on* g^2D. **(d)** *Two knots on* g^2D.

Figure 8: *Crafting a physical realization as temari.* ***(a)*** *temari with pins at the dodecahedron vertices and help-lines of the projected dodecahedron;* ***(b)*** *added pins to guide a single knot on* g^2D; ***(c)*** *filling in a single knot on* g^2D; ***(d)*** *adding a second knot on* g^2D.

contains such a crossing. Then, the first knot is placed between the pins, see Figure 8c. Subsequent knots are added similarly, see Figure 8d.

Finally, Figure 7 shows realizations of the weaving structures of the first three iterative applications of the *gyro* operation to the dodecahedron. That is, the temari show the link diagram of the weaving structures as they arise on gD, g^2D, and g^3D. The canvas balls are made from fabric covered with cotton yarn and decorated with links made from cotton embroidery thread. They have a diameter of 4.1 cm, 5.9 cm, and 9.2 cm, respectively. We choose black canvas balls to provide a neutral grounding with maximal contrast to the predominantly bright colors of the knots. The choice of the coloring scheme for the knots is guided by both a high contrast between the knots, in order to distinguish them well, and by a set of colors that provide a matching overall impression.

The colored knots are framed with black threads to emphasize the link structure and to highlight the crossings. While crossings of two different knots are well recognizable because of the difference in colors, the black borders distinguish which part of the knot goes over or under in places where self-crossings occur, see the realizations of g^2D and g^3D in Figure 7. In the realizations mentioned before, black pentagonal areas stand out. Working with yarn, great circles, appear more stable than more curved arcs, which would be necessary to spread out the knots and their crossings more uniformly over the temari. While this can be achieved with more diligent and meticulous placement of supporting pins, for this piece, we do enjoy that the underlying icosidodecahedron shines through via its pentagons.

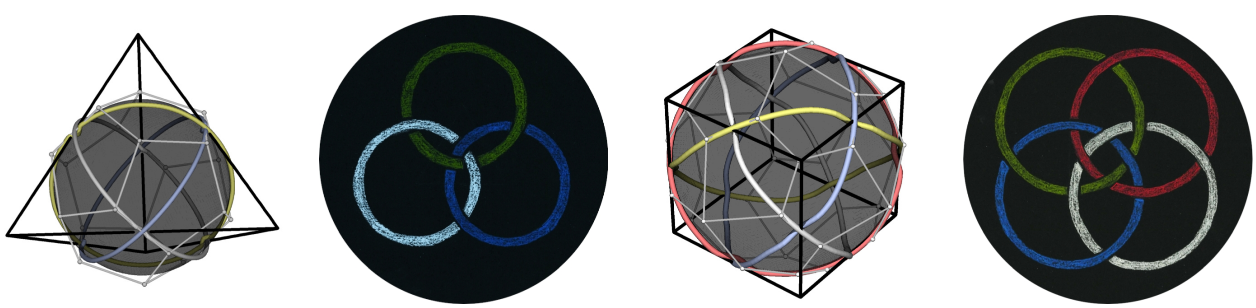

(a) *Knots on* gT=D. **(b)** *Link diagram of* gT=D. **(c)** *Knots on* gC. **(d)** *Link diagram of* gC.

Figure 9: *Weaving structure on* gT *and* gC *with the corresponding link diagrams.*

6 Extension to Further Solids

Our initial choice of applying the *gyro* operation to the dodecahedron was arbitrary in the sense that it can be applied to any solid. Thus, a natural question is, whether the observations made on $\mathtt{g}^n\mathtt{D}$, regarding the number of knots in the link, carry over to other solids.

Taking the Platonic solids, it suffices to consider the tetrahedron T and the cube C, as the icosahedron and the octahedron are dual to the dodecahedron and the cube, respectively, and thus do not provide different weaving structures up to symmetrical changes. Counting the number of Petrie walks on the tetrahedron, we have three paths and indeed, on gT, there are three (un-)knots, see Figure 9a and the corresponding link diagram in Figure 9b. The Petrie walks on the tetrahedron have length 4, which coincides with the number of crossings of each knot on gT. Counting only the over-crossings—as those get replaced by link diagram Figure 6a—we get two, which is still even. After applying the *gyro* operation to the tetrahedron once more, we get two times five over-crossings, which is even and thus the knot splits into two knots of five over-crossings each. As the application of the *gyro* operation to the tetrahedron gives the dodecahedron, see Figure 9a, we have seen in the above that this number remains constant when applying the *gyro* operation iteratively to gT. A similar observation holds for the cube. Here, there are four Petrie walks and thus four knots on gC, see Figure 9a and the corresponding link diagram in Figure 9b. The Petrie walks on the cube have length six. If we, once more, focus only on the over-crossings, there are thus three, which is uneven. Hence, applying the *gyro* operation several times keeps the number of knots constant at four.

The scheme illustrated here provides the number of knots created on a given solid, after n-fold application of the *gyro* operation. This enables not only the creation of further, creative temari realizations, but also of corresponding renderings and link diagrams.

Acknowledgements

This research was partially funded by the Deutsche Forschungsgemeinschaft (DFG, German Research Foundation) – grant no. 455095046. It was supported by the cluster of excellence "Matters of Activity. Image Space Material" funded by the Deutsche Forschungsgemeinschaft (DFG, German Research Foundation) under Germany's Strategy-EXC 2025-390648296.

References

[1] B. A. Berken. "Ethnomathematics: unlocking the wonders of mathematical ideas." *82nd Annual Meeting of the National Council of Teachers of Mathematics*, 2004. http://www.snc.edu/math/docs/ethnomathematics.pdf.

[2] J. H. Conway, H. Burgiel, and C. Goodman-Strauss. "The Symmetries of Things." *CRC Press*, 2016.

[3] G. W. Hart. "Conway Notation for Polyhedra", 1998. https://www.georgehart.com/virtual-polyhedra/conway_notation.html.

[4] H. Lipschütz, U. Reitebuch, M. Skrodzki, and K. Polthier. "Weaving patterns inspired by the pentagon snub subdivision scheme." arXiv:2112.15057, 2021. https://arxiv.org/abs/2112.15057

[5] M. E. Watkins, J. L. Gross, and T. W. Tucker. "Infinite graphs and planar maps." *Encyclopedia of Mathematics and its Applications*, Cambridge University Press, 2009.

[6] C. Yackel. "Teaching Temari: Geometrically Embroidered Spheres in the Classroom." *Bridges Conference Proceedings*, Townson, Maryland, USA, July, 25–29, 2012, pp. 563–566. http://archive.bridgesmathart.org/2012/bridges2012-563.html.

[7] G. M. Ziegler. "Lectures on Polytopes." *Graduate Texts in Mathematics*, 152, Springer, 2006.